A silicon photomultiplier-based analog front-end for DC component rejection and pulse wave recording in photoplethysmographic applications

Simone Valenti
Department of Engineering
University of Palermo
Palermo, Italy
simone.valenti@unipa.it

Gabriele Volpes
Department of Engineering
University of Palermo
Palermo, Italy
gabriele.volpes@unipa.it

Antonino Parisi
Department of Engineering
University of Palermo
Palermo, Italy
antonino.parisi@unipa.it

Riccardo Pernice
Department of Engineering
University of Palermo
Palermo, Italy
riccardo.pernice@unipa.it

Salvatore Stivala
Department of Engineering
University of Palermo
Palermo, Italy
salvatore.stivala@unipa.it

Luca Faes
Department of Engineering
University of Palermo
Palermo, Italy
luca.faes@unipa.it

Alessandro Busacca
Department of Engineering
University of Palermo
Palermo, Italy
alessandro.busacca@unipa.it

***Abstract*— The growing attention towards healthcare and the constant technological innovations in the field of semiconductor components have allowed a widespread availability of smaller devices, suitable to be worn and able to continuously acquire physiological signals. Wearable devices are, however, more prone to yield signals corrupted by artifacts caused by movement. This issue is particularly relevant in photoplethysmographic (PPG) applications where also, to exploit the whole dynamic range of the acquisition device, the DC component of the signal should be removed and the AC component amplified. In this context, we have designed and realized an analog front-end (AFE) suitable to be integrated within PPG wearable devices able to minimize these problems by reducing the ambient light and the factors that can vary the average value of the current output from a silicon photomultiplier in a PPG system using a green LED. DC component elimination is pursued by a signal conditioning circuit realized by the design and the implementation of a transimpedance amplifier and a Miller integrator capable of following and subsequently subtracting the average value of the acquired signal, so as to obtain an output signal that fluctuates around zero. The step response of the feedback circuit was studied carrying out a PPG acquisition on wrist with promising preliminary results.**

Keywords*— *analog front-end (AFE), silicon photomultiplier (SiPM), photoplethysmography (PPG), bio-sensing applications, wearable health devices (WHD).

I. INTRODUCTION

The growing interest in healthcare and the unstoppable electronic miniaturization progress occurred during the last decade have pushed the scientific community to focus on the development of wearable biomedical devices able to monitor the individual's physiological state for improving quality of life, defined by World Health Organization (WHO) as a complete state of physical, mental and social well-being [1]. Wearable biomedical devices, also known as Wearable Health Devices, (WHD) are an emerging technology that assesses health quality performing a non-invasive continuous monitoring of a wide range of biosignals during daily-life routine, without undermining the subjects' comfort [2]. Thanks to the continuous research in the biomedical field, carried out in the last years by some of the biggest consumer electronics Companies (e.g. Apple, Samsung, Garmin, Xiaomi, Fitbit) [3], wearable devices have evolved rapidly and nowadays a large number of wearable solutions able to acquire parameters in different body districts is available [4]. Among them, with particular reference to wrist-based devices, it is worth mentioning Apple Watch, Samsung Watch and Xiaomi Smart Band, while as regards wearable devices on the abdomen, the HRM pro Garming band performs a daily-life evaluation of the heart status by acquiring cardiovascular parameters directly on the abdominal area. Moreover, recent advances in the field of flexible sensors and wearable electronics have allowed the creation of non-invasive devices, able to acquire physiological signals locally on the body by adhering perfectly to the skin, minimizing movement artifacts and thus improving the quality of the data acquired [5]-[7]. Important physiological parameters, such as body temperature, motion characteristics, oxygen saturation and heart rate [8] can be monitored by using WHD. The data collected can be exchanged in the cloud, creating a network of biomedical devices known as Internet of Medical Things (IoMT) and allowing, e.g., an early detection of pathological conditions or a constant monitoring of ongoing diseases, in perspective lightening the load on health-care systems for the follow-up of both elderly and frail subjects [9].

With a percentage of elderly people expected to grow over the years (it is estimated that more than 20% of the population will be 65 years and older by 2050 [10]), the rate of people suffering from cardiovascular disorders, such as arteriosclerosis, ischemic attack, arterial illness and heart failure will unceasingly increase, and such diseases will become one of the leading human causes of death in the world [11]. For these reasons, wearable devices which enable to acquire measures related to the cardiovascular system such as heart rate (HR), HR variability (HRV), blood pressure (BP) and percentage of blood oxygen saturation are crucial to monitor the onset of cardiovascular diseases and conditions that can lead to heart failure [12]–[14]. Instead of uncomfortable and bulky electrocardiography (ECG) equipment, most of the devices detecting this type of parameters nowadays take advantage of photoplethysmography (PPG), an optical technique, easy to apply, unexpensive and non-invasive, that is able to detect blood volume changes in the peripheral vessels at different body locations [14],[15]. The working principle of PPG is based on the fact that blood has a different light absorption coefficient compared to the surrounding tissues. The simplest PPG device is composed of a single LED illuminating the body district of interest through the emission of light at a specific wavelength (typically between 530 nm and 940 nm), and of a photodetector capturing reflected or transmitted light.

The acquired signal includes a variable part, i.e. an AC component, that is proportional to the change in blood vessels volume given by the cardiac cycle, which can be employed for extracting important cardiovascular parameters such as oxygenation, heart rate and its variability, blood pressure estimation, pulse transit time, pulse wave velocity a,nd pulse-to-pulse interval [14], [16]–[19]. The ease of use of PPG technique makes its use possible in different body districts: not only in the wrist, but also in the arm, neck and the sternum [15], [20]. The latter has been recently investigated in the literature for the detection of sleep apnea and sleep stages through the use of soft sternal patch PPG sensor [21]. Previous works have demonstrated that PPG signal can be employed as a surrogate of ECG to perform heart rate variability analysis [22]–[24], given the high degree of similarity with the indices extracted from ECG R-R intervals [19]. Nonetheless, the reliability of this signal is often affected by both the light reflected from the tissue surrounding the peripheral blood vessel and motion artifacts. These two conditions cause the PPG signal acquired by the photodetector to include a continuous (DC) or slowly varying component. Motion artifacts originates changes in DC component that, depending on the size of the movement, may cause the sensor saturation, resulting in a loss of arterial signal information [25], [26]. To limit this problem, it is necessary to design a system able to reduce this continuous component, making the acquisition less sensitive to motion artifacts and other disturbances that can increase the continuous component, thus obtaining a full-scale input range of the PPG signal. A partial solution to this problem is given by the choice of a green light emitting diode, since wavelengths around 530 nm are less sensitive to motion artifacts [27]. A second solution is given by the implementation of analog front ends with advanced filtering techniques that allow the elimination of the DC component [28], [29] , taking care to not delete parts of the useful signal during filtering. In the literature there are several works related to the implementation of electronic circuits for the DC component reduction. Most of them use medium-high complexity mixed signal circuits based on the double action of the ambient light elimination pursued by a switched-capacitor filter (that samples and subtracts the current output from the photodiode due to the ambient light), and DC compensation performed by a digital-to-analog converter [30]–[34]. Finally, recent research has been focused on the replacement of the photodiode with devices more performing in terms of photon acquisition, i.e. silicon photomultipliers (SiPM). These devices, due to their high intrinsic gain, allow to extend the optical acquisition sensitivity up to the single photon and to appreciate with greater details all the variations of the optical signal that affect the active surface of the device [35]. The higher resolution provided by this category of sensors allows to increase the AC/DC ratio of the signal.

In this perspective, in this work a new analog front-end (AFE) with DC component minimization has been designed and realized. The main difference between our solution and those present in the literature is that the DC component is reduced by exploiting a fully analog circuit, without the integration of additional digital components that increase circuit complexity, making our AFE suitable to be integrated within photoplethysmographic wearable PPG devices. The DC component minimization is pursued by a feedback circuit capable of following and subsequently subtracting the average value of the acquired signal. Finally, the step response of the circuit has been studied carrying out a preliminary PPG acquisition on the wrist in order to evaluate the proper functioning and the effective removal of the DC component. The preliminary experimental results are very promising, thus proving the potential usefulness of the system.

II. System Architecture

A. Photoplethysmographic waveform

A typical PPG signal acquired by a photodetector can be decomposed in both AC and DC components (Fig. 1). The first one represents the pulsatile component of the PPG waveform, which contains information related to instantaneous volume changes in blood vessels of a given body location and can be considered as a function of the cardiac cycle. In particular, it is a periodic waveform with a fundamental frequency at around 1 Hz (depending on the heart rate) and consists in a rising trend followed by a falling one, respectively related to the systolic and diastolic phases of the cardiac cycle. In high-resolution acquisition systems it is even possible to detect a particular change in the pulsatile component between the systolic and diastolic phases, known as dicrotic notch, which is a manifestation of aortic valve closure [15], [36]. The non-pulsatile component, which usually represents most of the total amplitude of the PPG signal, is instead mainly due to the presence of other tissues layers between the LED-photodetector interface, such as skin, veins and bias blood volume inside the arteries, which involve a constant absorption of the light beam, resulting in a continuous component (so called DC component) constantly detected by the photodetector [16].

Another factor that causes a considerable increase of the DC component, one of the problems of wearable photoplethysmographic devices, is the presence of ambient light accidentally acquired by the system, due to an incorrect positioning of the probe or even to small subject movements that excessively detach the photodetector from the body district where the signal is being acquired.

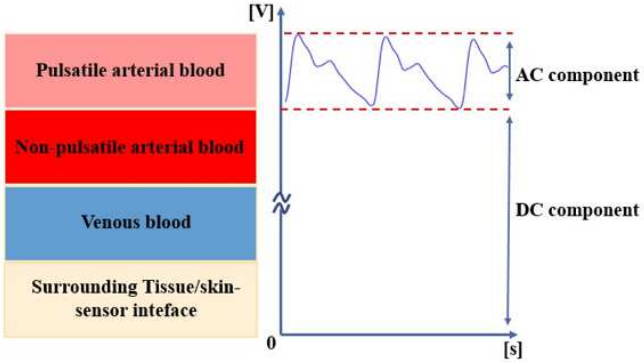

Fig. 1. Example of the path taken by the light beam from the skin interface up to the blood vessel for pulse wave detection. The AC component is caused by the variation of blood flow during the passage of the pulse wave, while the DC component is due to the constant absorption of light by other tissues (e.g. skin, venous blood and non-pulsatile component of the blood vessels) and also due to motion artifacts.

Since the DC component does not carry physiological information, it can be considered as a noise superimposed on the useful pulsatile component. For this reason, the main parameter used to characterize a photoplethysmographic device is the AC-to-DC ratio, which describes how the PPG signal is distributed between AC and DC components. Maximizing the AC-to-DC ratio (i.e. eliminating the DC component) is a requisite for the accurate acquisition of the

PPG signal, as it allows to obtain a full-range dynamic of the pulsatile component.

B. Circuit design

The circuit realized and used for the measurements performed in this work has been designed by Altium Designer Software and has been entirely assembled in our laboratories. It is possible to subdivide the entire area of the circuit into two main sub-areas: the first one related to signal transduction and to the power supply of the sensor, and the second one related to signal conditioning.

The first sub-area is formed by two main components engaged in the task of generating and detecting the light signal: the LED and the SiPM, respectively. The LED is a green OSRAM OS LT M673-P2R1-25 that emits photons at a wavelength of 532 nm and has an optical power at the interface of about 1 mW. The SiPM is an optical device that aims to acquire optical signals and convert them to a voltage signal suitable to be managed by an analog-to-digital converter (ADC). The SiPM employed in this work is sensitive to the single photon; it consists of an array of single photon avalanche diodes (SPAD) with a very high gain (of the order of 10^6), much higher than that of a common photodiode and that of an Avalanche Photodiode that are in the range of 10^2-10^3 [35], [37]. These characteristics are expected to produce significant improvements to the acquisition of PPG waveforms, as they allow to acquire signals with a reduced energy consumption and to achieve a higher AC/DC ratio, also guaranteeing high repeatability and better immunity to motion artifacts [38]. In previous works [18], [19], [39] we have employed a silicon photomultiplier supplied by STMicroelectronics with a breakdown voltage of about 28.0 V and a 3.5 mm × 3.5 mm active area (3600 microcells, 45% fill factor, and 58-µm cell pitch) enclosed in a 5-mm × 5.5-mm package. Responsivity measurements provided values ranging from 10^7 to 10^9 mA/W. In this work we have upgraded the device technology with a more performing silicon photomultiplier made by ONSEMI, the MICROJ 60035, which has an active area of 6.07 x 6.07 mm^2, 22.292 microcellles of SPAD and an intrinsic avalanche gain ranging from 2.9 to 6.3 x 10^6 [40]. This SiPM has a 75% geometric fill factor and is enclosed in a PCB with 5 pins (anode, cathode, ground, fast-output and a not-connected pin).

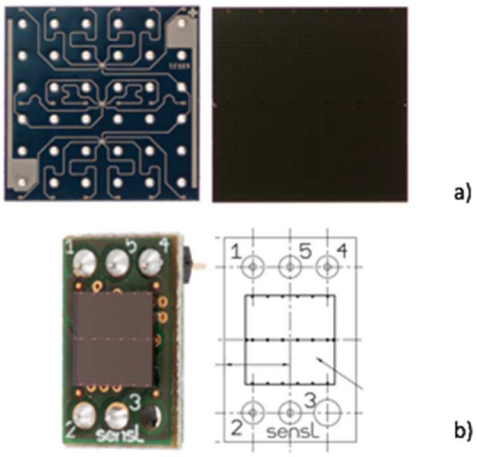

Fig. 2. SiPM MICROJ 60035: (a) bottom view and top view, (b) top view of the SMTPA board.

The chosen device has a breakdown voltage of about 24.5 V. The SiPM power supply was chosen very close to the breakdown region (with about 1 V of overvoltage) in order to ensure a good range of linearity [14].

Alongside with the employment of SiPM technology in place of conventional photodetectors, another main innovation of our front-end is the signal conditioning pipeline, which is composed of three parts, i.e. a transimpedance amplifier, an integrator, and a MOSFET transistor closed in a feedback loop. An operational amplifier was chosen for realizing the transimpedance amplifier (TIA). This component performs the task of transducing the current output from the SiPM, converting and amplifying it into a high-level voltage signal suitable to be conditioned. Furthermore, the virtual short circuit between the two input terminals of the operational amplifier makes both the photomultiplier DC operating point and its responsivity to remain fixed and independent on the current supplied by the same device. The feedback resistance of the TIA was chosen equal to 220 Ω; this condition, together with the fact that the current range supplied to the output from the photodetector ranges from 0 to 15 mA, causes the voltage signal to fluctuate between 0 and 3.3 V, making this configuration suitable to be implemented in a microcontroller system, in such a way to take advantage of the entire dynamics of an ADC. The voltage signal supplied by the transimpedance amplifier is put as input to a Miller integrator, made with an operational amplifier set in this configuration. The time constant of the integrator has been chosen in order to measure the average value of the signal directly at the output of this second block. The output of the integrator then goes to the gate of a MOSFET in triode configuration, in such a way to transform the information of the mean value into current that will be subtracted from the one going out from the photomultiplier; the signal entering the TIA is thus the PPG signal but shifted to zero. The output of the circuit is taken as the output of the transimpedance amplifier. The block diagram and the electrical schematic of the circuit are shown in Fig. 3.

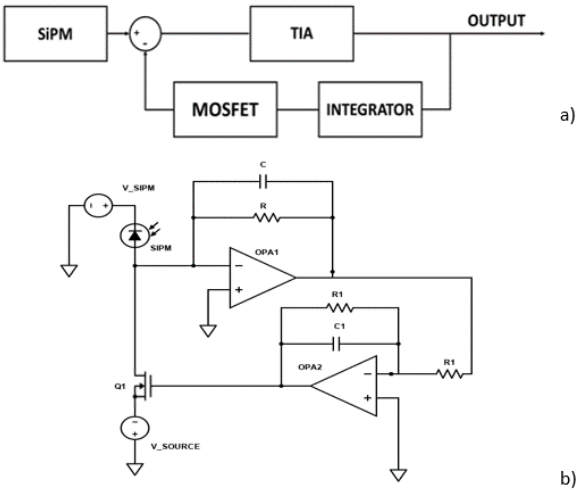

Fig. 3. Block diagram (a) and electrical schematic (b) of the circuit. The signal acquired by the SiPM is the input of the TIA, while the output is then put as the input of the integrator which extracts the mean value and brings it to the gate of the MOSFET that transforms this information into the current to be subtracted from the signal acquired by the photomultiplier.

C. Data acquisition and protocol

Measurements were carried out on the left wrist of a normotensive, healthy 26-years old male volunteer using a PPG probe (shown in Fig. 4) composed of the SiPM and the

green LED described in the previous sub-section. The full acquisition protocol lasts about 2 minutes, during which the sensor is intentionally exposed to ambient light with variable intensity. PPG measurements were carried out in reflectance mode and in indoor ambient lighting conditions. The SiPM and the LED were placed on a mask located directly on the PCB containing the entire signal conditioning circuit in such a way to ensure a fixed distance between the light source and the photodetector. A velcro band was used to ensure a suitable adhesion of the two devices to the wrist.

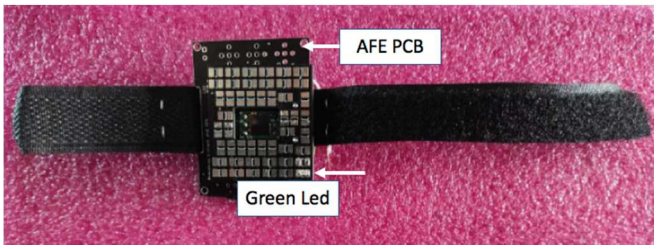

Fig. 4. PPG probe. The green LED is placed on a mask mounted on the PCB that contains the entire analog signal conditioning circuit.

The output signal from the transimpedance amplifier (which also represents the output of the entire circuit) has been acquired by a digital oscilloscope (Keysight DSOX3034T) with 8-bit vertical resolution. The signal was displayed in real-time on the oscilloscope screen and the step-response of the circuit was evaluated by introducing a forced additional input light source varying the DC component of the PPG pulse wave and consequently its average value. The signal was recorded at a sampling rate of 1 kHz and stored on a USB flash drive to carry out post-processing using MATLAB R2021b (The MathWorks, Inc., Natick, MA, USA) software.

III. Results and Discussion

Figure 5 shows a 4-seconds excerpt window of the PPG signal acquired using our system in open loop configuration (i.e. with the drain pin not connected to the SiPM anode), where the typical morphology of a wrist pulse wave is appreciable [34]. This waveform shows the main features that a PPG signal typically presents, showcasing the performance of our acquisition system. In this frame, in fact, it is easy to visually detect a systolic peak, followed by the dicrotic notch and, finally, the diastolic peak. An average continuous component of about -1.2 V and an alternate component of about 140 mV are present, thus obtaining an AC/DC ratio of about 0.12. The presence of a marked dicrotic notch, together with a high AC/DC ratio, demonstrates the high performance of our system in terms of resolution of the pulse wave, thus highlighting the utility of implementing a SiPM.

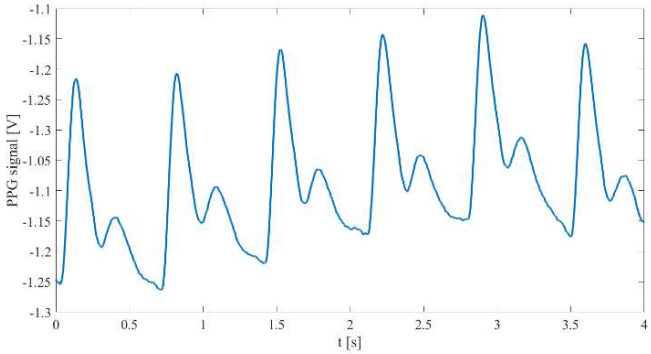

Fig. 5. A 4-second PPG signal acquisition window in open loop configuration.

In Fig. 6, the Fast Fourier Transform (FFT) of the signal is depicted, computed after the removal of DC component. As known, PPG is a periodic signal, and its period is exactly the average heart rate. Usually, a PPG signal has a useful bandwidth narrower if compared to the dynamics of an ECG signals: harmonics at frequencies higher than 15 Hz are usually neglectable [41], [42]; this is the reason why PPG pulse waves are commonly bandpass-filtered between 0.05 and 20 Hz [43]. The peak around 1.3 Hz represents the heart rate, while other peaks at higher frequencies (2.6, 3.9 Hz) are the second and third harmonics, respectively. The small peak around 0.2 Hz corresponds to breathing. PPG and ECG signals include frequency content of importance for diagnostic purposes up to 15 Hz for PPG and 250 Hz for ECG, respectively.

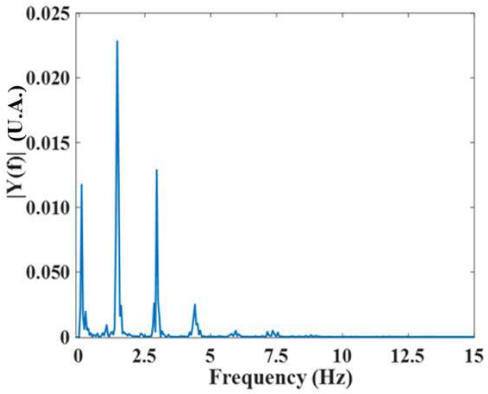

Fig. 6. Fast Fourier Transform (FFT) of the PPG signal acquired on the wrist.

Therefore, the readout circuit has to guarantee amplification of the signals within this bandwidth, with a good signal-to-noise ratio, and rejection of non-biological or extraneous signals.

Figure 7 depicts the step response following the introduction of a forced light source when the feedback loop is closed (a) and when it is open (b). The source is a white LED and is aimed at simulating an instantaneous increase of the ambient light, in the environment surrounding our circuit. The light step is introduced after a few seconds, in order to stress the system during the pulse wave acquisition. Afterwards, the signal is switched off again to evaluate the behavior of the system in response to the return to the initial lighting conditions. Analyzing the open loop response (Fig. 7a), the system in the first 2.7 seconds, is carrying out a continuous acquisition of the PPG signal with indoor ambient light conditions. This pulse signal has a DC average component of about -2.02 V and a pulsatile AC component of about 60 mV identifying an AC/DC ratio of 0.03. Soon after the introduction of the light step, the system responds with a downward shift (since the TIA inverts the signal) increasing the DC value of the acquired signal proportionally to the additional amount of light introduced into the environment and consequently captured by the photodetector. At 7.8 seconds the additional light source is removed and the system returns to its initial condition. It is easy to deduce from this figure how the AC/DC ratio is completely dependent also on the amount of ambient light present at the time of measurement, given that this ratio drops to 0.02 when the step of light is present in the system.

Analyzing the closed loop response (Fig. 7b) to the application of the step, after a small transitory, where the information content is preserved, the system responds shifting to the initial mean value by effectively eliminating (discarding) the DC component introduced by the light signal, minimizing the disturbance introduced by the new ambient light conditions. The same behavior of the system is found at the extinction of the light step, confirming the expected results of the designed circuit.

It is also important to note that the peak-to-peak value of the wave is reduced by about 1/3 compared to the open-loop signal obtained, in favor, however, of an AC/DC ratio much higher than about 0.25.

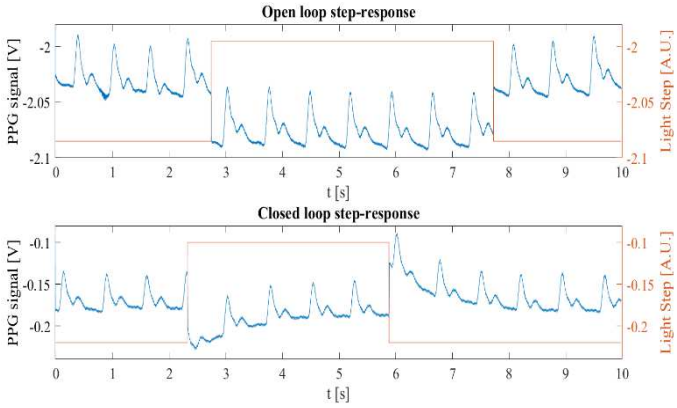

Fig. 7. A 4-second PPG signal acquisition window (blue graph) in open and closed loop configuration during the step-response consisting of two different ambient light conditions (red curve).

IV. CONCLUSION

An analog front-end designed for effectively cancelling both the ambient light and non-pulsatile pulse wave DC components has been designed and implemented. The use of a high intrinsic responsivity photodetector such as the SiPM as an alternative to the traditional photodiode, together with the reduction of the continuous component carried out by the feedback circuit, allows to obtain an output signal where the pulsatile part of the PPG signal is enhanced, enabling to better exploit the dynamics of the analog-to-digital conversion circuit for signal acquisition.

The results of our preliminary measurements highlight the remarkable resolution of the pulse wave obtained from the build PPG probe, in which the typical morphological characteristics acquired from the wrist are clearly distinguishable, such as the visual distinctions of the pulse-to-pulse interval (PPI) and dicrotic notch, the latter only detectable in high resolution PPG acquisition systems. Furthermore, the step response carried out during the measurements demonstrates the proper working of the feedback circuit, confirming the expected results in the design stage and validating the system and its use in biomedical devices requiring the DC component elimination in the pulse wave signal.

Preliminary measurements carried out moving the left arm to simulate typical physical activity conditions have shown the feasibility of the proposed AFE to reduce also motion artifacts. The preliminary results are not shown here for brevity and should be validated in a future work after further measurements.

Finally, the described system allows to detect an improved pulsatile component (i.e. AC component) that, together with the minimum cost and size of the device, make it suitable to be easily integrated into wearable devices framed in the field of the Internet of Medical Things and designed to perform physiological monitoring.

Future works should concern the characterization of the AFE in terms of bandwidth, AC/DC ratio, ambient light response in different physical conditions, to show its robustness in case of an incorrect positioning of the device on the body or in presence of various ambient light conditions at different times during the day, or finally its immunity to motion artifacts.

Furthermore, it might be interesting to upgrade the device by encapsulating it into a soft matrix in order to isolate the system from the surrounding environment. In perspective, it will be fundamental to realise a single device – integrating also the microcontroller alongside with the signal conditioning circuit, the LED diode and the photodetector, in order to make the measurements on the wrist and directly preprocess in real-time the data, also saving them on an internal memory or sending the results and the extracted parameters to other devices using low-energy wireless communication technologies (e.g. Bluetooth Low Energy).

ACKNOWLEDGMENT

SV Ph.D. grant was supported by the Italian MIUR PON R&I 2014-2020 “Dottorati innovativi con caratterizzazione industriale” funding programme. GV Ph.D. grant was supported by Istituto Nazionale Previdenza Sociale (INPS) Ph.D. fellowship, project title “Sviluppo di protocolli sperimentali e impiego di soluzioni tecnologiche finalizzate alla valutazione oggettiva e quantitativa dello stress lavoro-correlato”. RP was supported by the Italian MIUR PON R&I 2014-2020 AIM project no. AIM1851228-2. We kindly thank the support of PO PSN project no. 2017/4.1.14 and of Dr. Salviato and Dr. Carruba (ARNAS Ospedali Civico Di Cristina-Benfratelli, Palermo, Italy), and of Italian Ministry of Education, University and Research “Sensoristica intelligente, infrastrutture e modelli gestionali per la sicurezza di soggetti fragili” (4FRAILTY) project (PON R&I ARS01_00345).

REFERENCES

[1] “Constitution of the World Health Organization”, American Journal of Public Health and the Nations Health 36, no. 11 (November 1, 1946).

[2] D. Dias and J. P. S. Cunha, “Wearable health devices—vital sign monitoring, systems and technologies,” Sensors (Switzerland), vol. 18, no. 8. MDPI AG, Aug. 01, 2018. doi: 10.3390/s18082414.

[3] M. Altini and L. E. Dunne, “What’s Next for Wearable Sensing?,” IEEE Pervasive Computing, vol. 20, no. 4, pp. 87–92, 2021, doi: 10.1109/MPRV.2021.3108377.

[4] K. Ueafuea *et al.*, “Potential Applications of Mobile and Wearable Devices for Psychological Support during the COVID-19 Pandemic: A Review,” *IEEE Sens. J.*, vol. 21, no. 6, pp. 7162–7178, 2021, doi: 10.1109/JSEN.2020.3046259.

[5] M. Guess, N. Zavanelli, and W. H. Yeo, “Recent Advances in Materials and Flexible Sensors for Arrhythmia Detection,” *Materials (Basel).*, vol. 15, no. 3, 2022, doi: 10.3390/ma15030724.

[6] Y. Khan *et al.*, “A flexible organic reflectance oximeter array,” *Proc. Natl. Acad. Sci. U. S. A.*, vol. 115, no. 47, pp. E11015–E11024, 2018, doi: 10.1073/pnas.1813053115.

[7] H. Kim *et al.*, “Fully Integrated, Stretchable, Wireless Skin-Conformal Bioelectronics for Continuous Stress Monitoring in Daily Life,” *Adv. Sci.*, vol. 7, no. 15, pp. 1–10, 2020, doi: 10.1002/advs.202000810.

[8] R. S. Bisht, S. Jain, and N. Tewari, “Study of Wearable IoT devices in 2021: Analysis Future Prospects,” in Proceedings of 2021 2nd International Conference on Intelligent Engineering and Management, ICIEM 2021, Apr. 2021, pp. 577–581. doi:

10.1109/ICIEM51511.2021.9445334.
[9] S. Vishnu, S. R. Jino Ramson, and R. Jegan, "Internet of Medical Things (IoMT)-An overview," in ICDCS 2020 - 2020 5th International Conference on Devices, Circuits and Systems, Mar. 2020, pp. 101–104. doi: 10.1109/ICDCS48716.2020.243558.
[10] R. J. Mitchell, S. R. Lord, L. A. Harvey, and J. C. T. Close, "Obesity and falls in older people: Mediating effects of disease, sedentary behavior, mood, pain and medication use," Archives of Gerontology and Geriatrics, vol. 60, no. 1, pp. 52–58, Jan. 2015, doi: 10.1016/j.archger.2014.09.006.
[11] P. Kakria, N. K. Tripathi, and P. Kitipawang, "A real-time health monitoring system for remote cardiac patients using smartphone and wearable sensors," International Journal of Telemedicine and Applications, vol. 2015, 2015, doi: 10.1155/2015/373474.
[12] T. D. Bradley and J. S. Floras, "Sleep apnea and heart failure: Part I: Obstructive sleep apnea," Circulation, vol. 107, no. 12. pp. 1671–1678, Apr. 01, 2003. doi: 10.1161/01.CIR.0000061757.12581.15.
[13] T. Kasai, "Sleep apnea and heart failure," Journal of Cardiology, vol. 60, no. 2. pp. 78–85, Aug. 2012. doi: 10.1016/j.jjcc.2012.05.013.
[14] D. Agro et al., "PPG embedded system for blood pressure monitoring," Jan. 2015. doi: 10.1109/AEIT.2014.7002012.
[15] J. Allen, "Photoplethysmography and its application in clinical physiological measurement," Physiological Measurement, vol. 28, no. 3. Institute of Physics Publishing, Mar. 01, 2007. doi: 10.1088/0967-3334/28/3/R01.
[16] Y. Maeda, M. Sekine, and T. Tamura, "The advantages of wearable green reflected photoplethysmography," in Journal of Medical Systems, Oct. 2011, vol. 35, no. 5, pp. 829–834. doi: 10.1007/s10916-010-9506-z.
[17] D. N. Dutt and S. Shruthi, "Digital processing of ECG and PPG signals for study of arterial parameters for cardiovascular risk assessment," in 2015 International Conference on Communication and Signal Processing, ICCSP 2015, Nov. 2015, pp. 1506–1510. doi: 10.1109/ICCSP.2015.7322766.
[18] D. Oreggia et al., "Physiological parameters measurements in a cardiac cycle via a combo PPG-ECG system," 2015. doi: 10.1109/AEIT.2015.7415214.
[19] R. Pernice, A. Parisi, G. Adamo, S. Guarino, L. Faes, and A. Busacca, "A portable system for multiple parameters monitoring: towards assessment of health conditions and stress level in the automotive field," in 2019 AEIT International Conference of Electrical and Electronic Technologies for Automotive (AEIT AUTOMOTIVE), 2019, pp. 1–6.
[20] Y. Zhong, Y. Pan, L. Zhang, and K. T. Cheng, "A wearable signal acquisition system for physiological signs including throat PPG," *Proc. Annu. Int. Conf. IEEE Eng. Med. Biol. Soc. EMBS*, vol. 2016-Octob, no. c, pp. 603–606, 2016, doi: 10.1109/EMBC.2016.7590774.
[21] N. Zavanelli et al., "At-home wireless monitoring of acute hemodynamic disturbances to detect sleep apnea and sleep stages via a soft sternal patch," 2021.
[22] R. Pernice et al., "Comparison of short-term heart rate variability indexes evaluated through electrocardiographic and continuous blood pressure monitoring," Medical and Biological Engineering and Computing, vol. 57, no. 6, pp. 1247–1263, Jun. 2019, doi: 10.1007/s11517-019-01957-4.
[23] R. Pernice et al., Reliability of short-term heart rate variability indexes assessed through photoplethysmography. In 2018 40th Annual International Conference of the IEEE Engineering in Medicine and Biology Society (EMBC) (pp. 5610-5513). IEEE.
[24] A. Schäfer and J. Vagedes, "How accurate is pulse rate variability as an estimate of heart rate variability?: A review on studies comparing photoplethysmographic technology with an electrocardiogram," International Journal of Cardiology, vol. 166, no. 1. pp. 15–29, Jun. 05, 2013. doi: 10.1016/j.ijcard.2012.03.119.
[25] H. Han and J. Kim, "Artifacts in wearable photoplethysmographs during daily life motions and their reduction with least mean square based active noise cancellation method," Computers in Biology and Medicine, vol. 42, no. 4, pp. 387–393, Apr. 2012, doi: 10.1016/j.compbiomed.2011.12.005.
[26] K. A. Reddy, B. George, and V. J. Kumar, "Use of Fourier series analysis for motion artifact reduction and data compression of photoplethysmographic signals," in IEEE Transactions on Instrumentation and Measurement, 2009, vol. 58, no. 5, pp. 1706–1711. doi: 10.1109/TIM.2008.2009136.
[27] J. Lee, K. Matsumura, K. I. Yamakoshi, P. Rolfe, S. Tanaka, and T. Yamakoshi, "Comparison between red, green and blue light reflection photoplethysmography for heart rate monitoring during motion," in Proceedings of the Annual International Conference of the IEEE Engineering in Medicine and Biology Society, EMBS, 2013, pp. 1724–1727. doi: 10.1109/EMBC.2013.6609852.
[28] F. Marefat, R. Erfani, and P. Mohseni, "A 1-V 8.1-μ W PPG-Recording Front-End with > 92-dB DR Using Light-to-Digital Conversion with Signal-Aware DC Subtraction and Ambient Light Removal," IEEE Solid-State Circuits Letters, vol. 3, no. 1, pp. 17–20, Dec. 2020, doi: 10.1109/LSSC.2019.2957261.
[29] J. Kim, T. Lee, J. Kim, and H. Ko, "Ambient light cancellation in photoplethysmogram application using alternating sampling and charge redistribution technique," in Proceedings of the Annual International Conference of the IEEE Engineering in Medicine and Biology Society, EMBS, Nov. 2015, vol. 2015-November, pp. 6441–6444. doi: 10.1109/EMBC.2015.7319867.
[30] Jongpal Kim, Takhyung Lee, Jihoon Kim, and Hyoungho Ko, "Ambient Light Cancellation in Photoplethysmogram Application Using Alternating Sampling and Charge Redistribution Technique," 2015.
[31] F. Marefat, R. Erfani, and P. Mohseni, "A 1-V 8.1-μ W PPG-Recording Front-End with > 92-dB DR Using Light-to-Digital Conversion with Signal-Aware DC Subtraction and Ambient Light Removal," IEEE Solid-State Circuits Letters, vol. 3, no. 1, pp. 17–20, Dec. 2020, doi: 10.1109/LSSC.2019.2957261.
[32] Q. Lin et al., "A 134 DB Dynamic Range Noise Shaping Slope Light-to-Digital Converter for Wearable Chest PPG Applications," IEEE Transactions on Biomedical Circuits and Systems, vol. 15, no. 6, pp. 1224–1235, Dec. 2021, doi: 10.1109/TBCAS.2021.3130470.
[33] Q. Lin et al., "A 119dB Dynamic Range Charge Counting Light-to-Digital Converter for Wearable PPG/NIRS Monitoring Applications," IEEE Transactions on Biomedical Circuits and Systems, vol. 14, no. 4, pp. 800–810, Aug. 2020, doi: 10.1109/TBCAS.2020.3001449.
[34] Ryosuke Yabuki et al., "PPG and SpO2 Recording Circuit with Ambient Light Cancellation for Trans-Nail Pulse-Wave Monitoring System," 2019.
[35] G. Adamo et al., "Signal to Noise Ratio of silicon photomultipliers measured in the continuous wave regime," in 2014 Third Mediterranean Photonics Conference, 2014, pp. 1–3. doi: 10.1109/MePhoCo.2014.6866473.
[36] M. Teresa Politi et al., "The dicrotic notch analyzed by a numerical model", doi: 10.1016/j.compbiomed.2016.03.005ï.
[37] M. Mazzillo et al., "Silicon photomultipliers with embedded optical filters for wearable healthcare applications," in 2017 IEEE SENSORS, 2017, pp. 1–3. doi: 10.1109/ICSENS.2017.8234373.
[38] M. Mazzillo et al., "Silicon photomultiplier technology at STMicroelectronics," in IEEE Transactions on Nuclear Science, Aug. 2009, vol. 56, no. 4, pp. 2434–2442. doi: 10.1109/TNS.2009.2024418.
[39] R. Pernice et al., "Low invasive multisensor acquisition system for real-time monitoring of cardiovascular and respiratory parameters," in 2020 IEEE 20th Mediterranean Electrotechnical Conference (MELECON), 2020, pp. 306–310. doi: 10.1109/MELECON48756.2020.9140716.
[40] onsemi, "MICROJ-SERIES - Silicon Photomultipliers (SiPM), High PDE and Timing Resolution Sensors in a TSV Package." [Online]. Available: www.onsemi.com
[41] F. Rundo, C. Spampinato, and S. Conoci, "Ad-hoc shallow neural network to learn hyper filtered photoplethysmographic (PPG) signal for efficient car-driver drowsiness monitoring," Electronics (Switzerland), vol. 8, no. 8, Aug. 2019, doi: 10.3390/electronics8080890.
[42] M. Elgendi, I. Norton, M. Brearley, D. Abbott, and D. Schuurmans, "Detection of a and b waves in the acceleration photoplethysmogram," 2014. [Online]. Available: http://www.biomedical-engineering-online.com/content/13/1/139
[43] J. Allen, K. Overbeck, G. Stansby, and A. Murray, "Photoplethysmography assessments in cardiovascular disease," 2006. [Online]. Available: www.instmc.org.uk